

## DEVELOPMENT OF A TEST DEVICE FOR THE EVALUATION OF JOURNAL BEARINGS

K. SANDVIK<sup>1</sup>, A. LEHTOVAARA<sup>1\*</sup>, E. MAKKONEN<sup>1</sup>, M. KALLIO<sup>2</sup>, K. KUVAJA<sup>2</sup>,  
V-T. KUOKKALA<sup>3</sup>.

<sup>1</sup>Tampere University of Technology, Mechanics and Design  
P.O.Box 589, FIN-33101 Tampere, Finland

\*Corresponding author: arto.lehtovaara@tut.fi

<sup>2</sup>Metso Minerals, P.O.Box 306, FIN-33101 Tampere, Finland

<sup>3</sup>Tampere University of Technology, Materials Science,  
Tampere Wear Center, P.O.Box 589, FIN-33101 Tampere, Finland

### ABSTRACT

Journal and thrust bearings are widely used in heavy industry. Today, there is a growing need for studying different kinds of new bearing material and coating solutions in operating conditions where full film lubrication cannot be achieved or sustained. A test device for the evaluation of journal bearings was developed. The device consists of a rotating shaft and four stationary test bearings. This scheme eliminates the need for support bearings, allowing an accurate measurement of friction. The initial tests were carried out with a variety of loads and sliding speeds in mixed and full film regimes. The friction results in the form of a Stribeck curve were obtained and found to be in line with general trends. The results also indicate that the bearing lift-off speed occurs when the value of the non-dimensional  $\eta_e n / p_{pro}$  - parameter is in the range of  $0.5 \cdot 10^{-8}$  -  $1.0 \cdot 10^{-8}$ .

Keywords: hydrodynamic lubrication, journal bearings, test device, friction

### INTRODUCTION

Journal and thrust bearings are widely used in heavy industry. The main advantages of these bearings are their very low friction coefficient and no-wear conditions, when they operate with full film lubrication. Further, they allow transient loading and they withstand dirty operating conditions, which makes them very suitable, for example, for stone crusher applications. However, challenges may appear when full film lubrication cannot be achieved or sustained. This occurs at low sliding velocities combined with high loading, which become increasingly evident if bearing start and stop actions are introduced under loaded conditions. Other possible reasons are interruptions in the oil feed and shaft misalignment. These operating conditions leads to mixed or boundary lubrication conditions, where the load is partially (mixed)

or totally (boundary) carried by surface asperities. In boundary lubrication conditions, prevention of total metal-to-metal adhesion between surfaces may be enhanced by very thin (molecular level) reaction layers formed by lubricant additives. The role of these materials and lubricant properties are clearly important under these operating conditions. The lubrication conditions in sliding bearings can often be represented by a Stribeck curve, which shows that the lubrication conditions strongly affect the friction coefficient and the damage risk to the sliding bearing. The theoretical aspects and main properties of hydrodynamic journal bearings can be found, for example, in [1- 3].

The three-dimensional transient models for the hydrodynamic lubrication of journal and thrust bearings have been developed on the basis of the Reynolds equation. The journal

bearing model includes features such as thermal effects, shaft misalignment, axial lubricant supply groove, varying bearing geometry and the non-flooded oil inlet flow [4]. The test device for the evaluation of thrust bearings has already been developed and the results were confirmed by comparison with the numerical thrust bearing model [5]. The models are formulated in such a way that they can be applied in common engineering practice in industries requiring a reasonably fast and easily applicable model. More complex numerical models also exist, but they may not yet be part of common engineering practice in industry. However, experimental testing is clearly needed for verifying the numerical model for journal bearings and for defining realistic input values for the model.

Today, there is a growing need for study of different kinds of new bearing material and coating solutions in operating conditions where full film lubrication cannot be achieved or sustained. This calls for experiments in mixed and boundary lubrication conditions. For example, in the most demanding applications, such as stone crushers, lead is used in a bearing material because of its superior dry lubrication and embedding properties as well as its toleration of shaft misalignment. However, lead is an environmental and occupational hazard at all stages of the product lifespan. The European Union has taken steps to ban the use of lead, thus creating a need for a substitute. Finding lead-free or low lead content bearing materials is challenging and expensive and it will inevitably involve field tests to validate promising substitute materials. Before this stage is reached, laboratory scale tests will be needed for screening purposes.

Various types of devices for testing journal bearings on a laboratory scale have been developed, for example in [6-8]. In addition to a test bearing unit and frame, the other main components are normally loading, drive, lubrication, control and measuring systems. The test bearing unit typically consists of one

test bearing, its housing together with a shaft and support bearings. A comprehensive description of a laboratory test rig and in particular the instrumentation for testing a hydrodynamic thrust bearing is given in [9]. A survey of experimental data for fixed geometry hydrodynamic journal bearings is given in [10].

In this study, the development of a test device for the evaluation of journal bearings under a variety of lubrication regimes is described. In addition, the initial friction results obtained with test device are shown in the form of a Stribeck curve and then discussed.

## HYDRODYNAMIC JOURNAL BEARINGS

In this study, a journal bearing consists of a rotating shaft within a stationary bearing (bushing), as shown in Fig. 1. The circular bearing includes an axial lubricant supply groove.

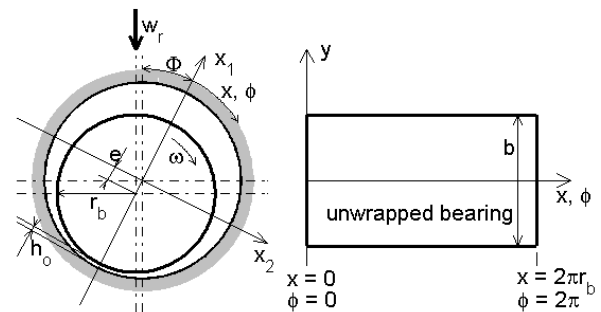


Figure 1. Illustration of hydrodynamic journal bearing.

In steady-state operating conditions, the load-induced shaft eccentricity with the bush allows the converging wedge-shaped geometry of the lubricant film which, together with the shaft rotation, produces the load supporting hydrodynamic film. The degree of eccentricity adjusts itself until the load is balanced by the pressure generated in the converging lubricant film. The line of centers ( $x_1$ ), where the minimum and maximum film thicknesses are located, is inclined to the load line at the attitude angle  $\Phi$ . This angle is

dependent on the operating conditions. In a transient case, a squeeze film effect may also momentarily maintain the lubrication film. Fig. 1 also shows an unwrapped journal bearing, length  $2\pi r_b$  and width  $b$ .

The solution of the hydrodynamic lubrication equations between the shaft and bearing is based on the Reynolds equation. Allowing for side leakage, assuming a Newtonian lubricant and neglecting fluid inertia effects, the transient Reynolds equation for an incompressible lubricant is:

$$\frac{\partial}{\partial x} \left( h^3 \frac{\partial p}{\partial x} \right) + \frac{\partial}{\partial y} \left( h^3 \frac{\partial p}{\partial y} \right) = 6\eta_e u_b \frac{\partial h}{\partial x} + 12\eta_e \frac{\partial h}{\partial t} \quad (1)$$

with the condition  $p \geq 0$  in the domain and  $p = 0$  at the boundaries. Film thickness  $h$  and pressure distribution  $p$  can be solved numerically from the Reynolds equation, where  $u_b$  is the sliding speed and  $\eta_e$  the effective viscosity.

Friction force  $F_b$  in the x-direction is calculated by integrating the shear stress of the lubricant over the bearing area:

$$F_b = \int_{-b/2}^{b/2} \int_0^{2\pi r_b} \left( \frac{h}{2} \frac{dp}{dx} + \frac{\eta_e u_b}{h} \right) dx dy \quad (2)$$

The corresponding friction coefficient  $f$  and power loss  $h_p$  can be expressed as:

$$f = \frac{F_b}{w_r} \quad (3)$$

$$h_p = F_b u_b \quad (4)$$

Assuming that a proportion  $K$  of the total heat generated by friction is carried away by the lubricant, the maximum temperature rise of the lubricant  $\Delta T$  is given as [3]:

$$\Delta T = \frac{2Kh_p}{\rho c_p q_{in}} \quad (5)$$

where  $q_{in}$  represents lubricant flow to the bearing. The effective temperature  $T_e$  within the lubricant is approximated by the equation:

$$T_e = T_{in} + \Delta T / 2 \quad (6)$$

The effective viscosity in the bearing is determined from the effective temperature. A detailed description of the governing equations related to the modeling aspects of a hydrodynamic journal bearing is presented in reference [4].

## EXPERIMENTAL

### Test device

There is need for tests with different kinds of materials, coatings and surface topographies in mixed and boundary lubrication regime as well as tests to verify the hydrodynamic model in full film regime. This emphasizes the following features of the test device: a) the wide operating range across different lubrication regimes, b) an accurate friction measurement to establish the Stribeck curves and related bearing lift-off speeds c) a large enough bearing size to simulate large-scale bearings reasonably well, d) a versatile lubricant feed control and e) an advanced instrumentation.

The development process culminated in a test configuration, where a shaft is rotating within four stationary test bearings, as shown in Fig. 2. This scheme eliminates the usual need for support bearings, whose frictional effects must somehow be calibrated out from the shaft total torque. This may often be difficult and always includes a margin of error. In addition, a configuration with four test bearings in parallel gives more statistical information into the results since each bearing can also be monitored individually.

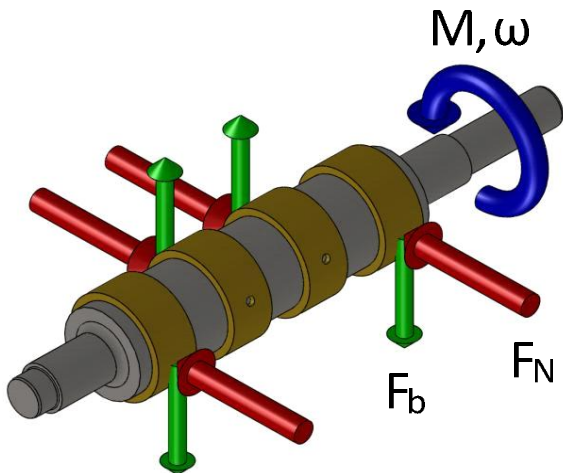


Figure 2. The shaft and bearings with the forces acting on them

The principle of the test device is shown in Fig. 3. An electric motor and a loading frame are bolted to the rigid main frame. The electric motor rotates the shaft, which is supported by four test bearings. A large electric motor coupled to a frequency converter permits variation of the rotation speed, and hence allows testing under all lubrication regimes. The load is applied with a hydraulic cylinder, which is connected to the loading frame. The applied load  $F_O$  affects the two middle bearings while an equal and opposite reaction force acts on the two bearings on the sides resulting in an equal loading  $F_N$  on all bearings. The housings of the test bearings are self-aligning eliminating the edge pressures typically caused by shaft misalignment and deflection. A lubrication unit is used to supply oil to each of the four test bearings through separate piping. The oil is fed to the bearings on the maximum clearance side. The angle between the axial lubrication groove and the direction of the normal loading can be adjusted from  $-40^\circ$  to  $40^\circ$ .

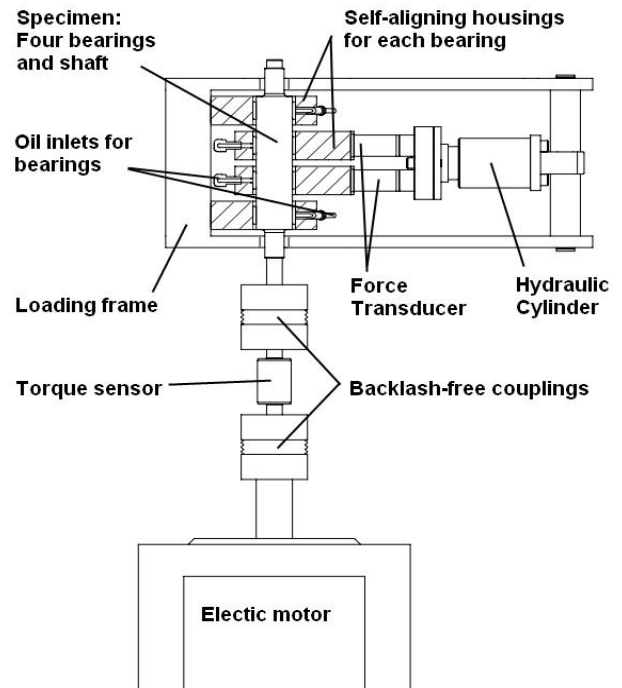


Figure 3. The test device as developed

The operational parameters, which are the normal load, the shaft rotation speed and the oil supply flow rate, temperature and pressure, are all monitored and can be adjusted continuously. The normal loading is measured with two parallel force cells. Identical force values in both cells also ensure that the loading is evenly distributed across the four test bearings. The load cell for measuring the driving torque, i.e. total frictional moment of the test bearings, is connected between the test and motor shafts via backlash-free couplings, which are rigid with respect to torsion, but which allow some bending. The friction coefficient  $f$  can be derived from the measured forces as follows:

$$f = \frac{M}{4r_b F_N} = \frac{M}{2r_b F_O} \quad (7)$$

where  $r_b$  is the radius of the shaft,  $F_N$  the load acting on each bearing,  $F_O$  the cylinder load and  $M$  the friction torque. The lubrication circuit and the related measurements are shown in Fig. 4.

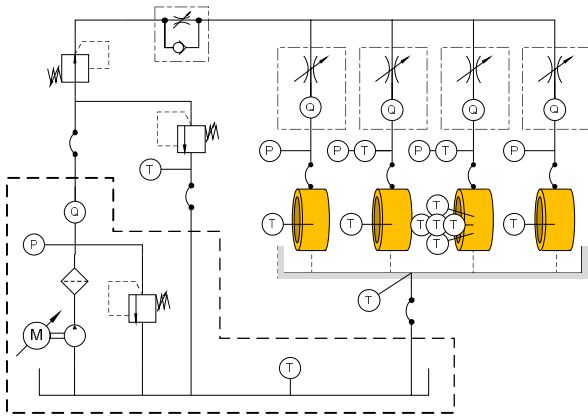


Figure 4. The lubrication chart and the location of temperature  $T$ , pressure  $P$  and flow rate  $Q$  measurements.

The total lubricant supply temperature, pressure, and flow rate can be measured from the output of the lubrication unit. The control of the lubricant tank, and hence the bearing inlet temperatures, is based on this temperature measurement. The lubricant is then fed to the test bearings, where these parameters are measured individually at the inlet to each bearing. Fine tuning of the flow rates is also enabled in order to achieve an equal flow rate in each bearing. The temperatures of each bearing back (the outer surface of bearing) can be measured at a specified location, so the performance of each bearing can be monitored individually in terms of frictional energy. These measurements are made in the pressurized zone of fluid film, typically at an angle of 20 degrees from the direction of normal load. One of the test bearing backs is also provided with four additional temperature detectors to follow the temperature distribution around the bearing. The detection of the oil outlet and the surrounding temperatures together with oil inlet temperatures and flow rates allow an estimation of the total heat transferred by the oil. All temperatures are measured with thermocouples.

#### Test bearings and shaft

A schematic view of the test bearing and the shaft is shown in Fig. 5. The test bearings

have inner diameters of 60 mm and a length of 30 mm. There is an axial oil supply groove on the inner surface of the bearing. The locations of the thermocouples in bearing 2 are shown in Fig. 5. In other bearings only the middle location is in use. The shaft is 60 mm in diameter, and length of the bearing surface is 229 mm, to accommodate four bearings with appropriate spacing.

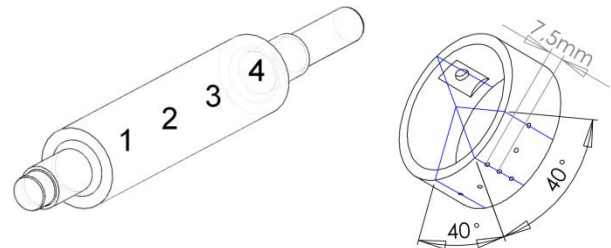


Figure 5. The test bearing and shaft with the locations of the bearings indicated 1 – 4.

Journal bearing performance is known to be sensitive for bearing clearance and roundness so particular attention was focused on measuring these critical bearing dimensions before the tests. In addition, the mean  $R_a$  roughness and the mean diameters were measured for each test bearing and shaft. The shaft surface roughness was measured at 27 points and for each bearing at 16 points. The inner diameters of the bearings were measured with 3-point micrometer after they had been installed in the housings. The value for the mean diameter of each bearing is based on 12 measurements. The variation in this diameter value with different  $\phi$  coordinate angles (Fig.1) indicates the degree of roundness of the bearing. Shaft diameters were measured with a micrometer at 12 points. The clearance is the difference between the mean value of the inner diameter of the bearing and mean value of the diameter of the shaft.

#### Test matrix

The aim of the initial tests was to determine the ability of the test device to meet the variety of load conditions. The test device was first heated by letting the lubricant

circulate through the device overnight under test temperature conditions. The friction torque meter was carefully calibrated before and after the tests. Three load levels were used with the projected pressures of 2, 6 and 12 MPa. Each loading was carried out at eight different sliding speeds, each step having a temperature stabilizing interval of 15 minutes. An average oil inlet pressure was kept at about 0.15MPa, which means that the oil inlet flow rate varies as a function of sliding speed. The angle between the axial lubrication groove and the direction of normal loading was 20°, i.e. the lubrication groove nearest to the point of the maximum clearance. The bearing back temperatures were measured at a point 180 degrees from the lubrication groove. The lubricant used was ISO VG 150 industrial gear oil. In this initial test, seals between the shaft and the loading frame were used. In later tests these seals were removed, which eliminates any external friction losses.

## RESULTS AND DISCUSSION

The tempered shaft material used in this study was 34CrNiMo6 and the bearings were made from CuSn10Pb10. The average bearing clearance was 172 µm and the average Ra roughness was 0.13 µm for the shaft and 0.34 µm for the bearings. The oil inlet temperature was 50 °C. The bearing back temperatures and friction coefficients as a function of time, with a loading of 6 MPa, are shown in Fig. 6.

Fig. 6 shows that at the lowest speed the friction coefficient is already high, which indicates that the bearings are operating in a mixed lubrication regime. During this load step, friction decreases which is due to the running-in of the bearing. As the sliding speed is increased, the minimum friction coefficient can be found in a controlled way. At this stage, the bearing back temperatures remained fairly constant and near the level of the oil inlet temperature. This indicates that frictional heat is high enough to cover the heat losses to the test device and to the surroundings. Further increases in sliding

speed gradually raise the friction coefficient showing that a full film hydrodynamic lubrication regime has been come into operation. Similarly, the bearing temperature increases along with frictional power loss as the sliding speed increases. Outer bearings 1 and 4 have very similar temperatures as do inner bearings 2 and 3. This indicates a very good match of operating and frictional conditions in each group. The slight temperature difference (less than three degrees) between these groups is due to the more efficient heat transfer from the outer bearings, and hence slightly reduced temperatures.

Increasing temperature trends at the end of the load steps at least in higher sliding speeds show that the stabilizing interval of 15 minutes is not enough to achieve complete steady-state operating conditions. Hence, the slight decreasing trend in friction can still be observed. However, the correct level of the friction coefficient in the full film regime was confirmed by the model results [4].

Friction behavior under different load conditions is shown in Fig. 7. The other load levels were also measured using a stabilizing interval of 15 minutes. Again, this is not enough to achieve complete steady-state operating conditions at all load stages.

Fig. 7 shows that the friction coefficient increases as the loading decreases, which is a known feature of hydrodynamic journal bearings. The increase in the friction coefficient as a function of sliding speed is due to the increasing shear rate of the lubricant. However, this increase in friction settles down at higher speeds as the increasing power loss raises temperatures in the bearings and hence decreases the effective viscosity. The results also indicate that the minimum friction coefficient occurs at low sliding speeds.

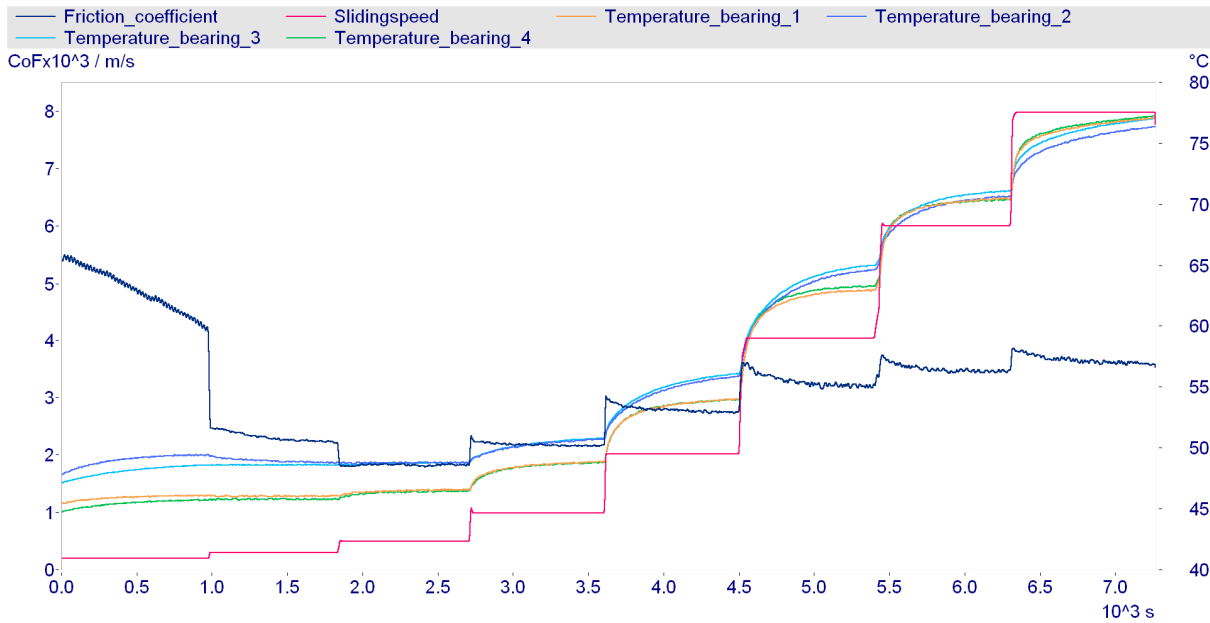


Figure 6. Friction coefficient  $f$ , sliding speed and bearing back temperatures as a function of time,  $p_{pro} = 6 \text{ MPa}$ .

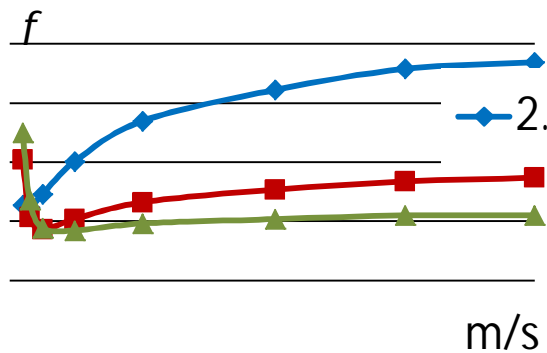


Figure 7. The frictional trend behavior at different load conditions as a function of sliding speed.

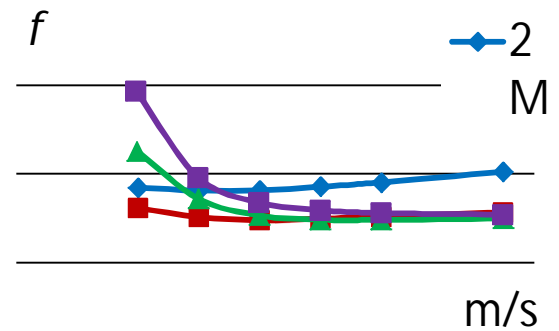


Figure 8. Friction coefficient at different loading conditions as a function of sliding speed.

The bearing lift-off speed, which corresponds to the location of the minimum friction coefficient, is of interest and merits further study. In this location, the transition from mixed to full film lubrication occurs so that the latter regime starts to dominate the friction process. The measurements were carried out with four load levels near the lift-off speed. Running-in of the surfaces was carried out before the test. The same sliding distance was used for each test point instead of having a constant running time. The results are shown in Fig. 8 as a function of sliding speed.

Fig.8 shows that the location of minimum friction coefficient, i.e. the bearing lift-off speed, increases as the projected pressure is increased. Under the operating conditions used, a very low friction coefficient can be achieved with sliding speeds as low as 0.1 m/s. Furthermore, the same friction results were mapped against the parameter  $\eta_e n / p_{pro}$ , where  $\eta_e$  is the effective viscosity,  $n$  is the rotational speed and  $p_{pro}$  the projected pressure. This is known as the Hersey number with the difference that the rotational speed is given here in revolutions per seconds. The results are shown in Fig. 9.

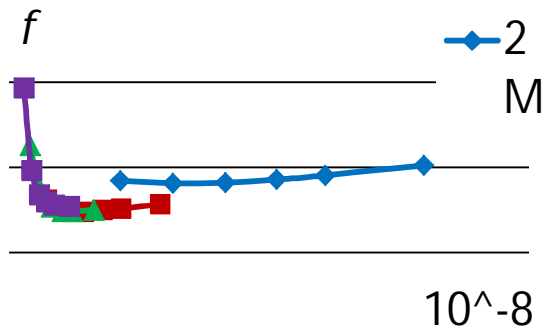


Figure 9. Friction coefficient against  $\eta_e n / p_{pro}$  - parameter.

Fig. 9 shows that this non-dimensional parameter is effective in consolidating the results measured with different loads, except for the lowest load. It may be that there is still some effect of running-in during this load stage. It is shown that hydrodynamic bearings can be operated with a friction coefficient as low as  $0.5 - 1.0E^{-8}$  in terms of the  $\eta_e n / p_{pro}$  - parameter. This is, at least, the case when the bearing operating conditions are free from effects of factors such as shaft misalignment. It is clear that the materials and surface roughness have an effect on the level of the observed bearing lift-off speed and the minimum friction coefficient.

## CONCLUSIONS

A test device for the evaluation of journal bearings was developed. The device consists of a rotating shaft and four stationary test bearings. This scheme eliminates the need for support bearings, allowing an accurate friction measurement. The housings of the test bearings are self-aligning which eliminates the edge pressures typically caused by shaft misalignment. The test device facilitates

flexible lubricant feed control and temperature as well as flow rate measurements in each test bearing. Determination of bearing clearance and roundness was based on conditions where the test bearings were already installed in their housings.

In the initial tests, the friction results in the form of Stribeck curves were obtained using a variety of loads and sliding speeds in mixed and full film regimes. The measured bearing temperatures were nearly uniform, indicating that the loading and friction conditions were fairly similar in each test bearing. The correct level of the friction coefficient in full film regime was initially verified with the model results. The results indicated that the non-dimensional parameter  $\eta_e n / p_{pro}$  fit well with the friction results measured at different loads and speeds. The bearing lift-off speed occurs when the value of this parameter is in the range between  $0.5 \cdot 10^{-8} - 1.0 \cdot 10^{-8}$ . This is at least the case when the bearing operating conditions are unaffected by factors such as shaft misalignment. In this study, this means that bearings could be operated with a low friction coefficient down to sliding speed levels of 0.1-0.2 m/s.

## ACKNOWLEDGEMENTS

The authors are grateful for the financial support provided by Metso Minerals Oy and Finnish Funding Agency for Technology and Innovation.

## REFERENCES

1. Hamrock, B., Fundamentals of Fluid Film Lubrication, McGraw-Hill, Inc, ISBN 0-07-025956-9, 1994, 690 p.
2. Stachowiak, G.W. and Batchelor, A.W., Engineering Tribology, Tribology Series, 24, Elsevier, 1993, The Netherlands, 872 p.
3. ESDU 66023, Calculation Methods for Steadily Loaded Pressure Fed Hydrodynamic Journal Bearings, (ESDU = Engineering Science Data Unit), London, 1982, 70 p.
4. Lehtovaara, A., A Numerical Model for Hydrodynamic Lubrication of Journal Bearings with Axial Lubricant Supply Groove and Axially Variable Geometry Finnish Journal of Tribology, 26 (2007) 3-14.
5. Pasanen, A., Kleemola, J. and Lehtovaara, A., Development of a Test Device for the Evaluation of Hydrodynamic Lubrication in Thrust Bearings, Finnish Journal of Tribology, 27 (2008) 12-20.
6. Valkonen, A., Oil Film Pressure in Hydrodynamic Journal Bearings, TKK Dissertations 196, Espoo 2009, 202 pp.
7. McCarthy, D.M.C., Glavatskih, S.B, Byheden, Å, Influence of Oil Type on the Performance Characteristics of a Two- Axial Groove Journal Bearing, Lubrication Science 21 (2009) 366-377.
8. Bouyer, J, Fillon, M., An Experimental Analysis of Misalignment Effects on Hydrodynamic Plain Journal Bearing Performances, Journal of Tribology 124 (2002) 313-319.
9. Glavatskih, S.B, Laboratory Research Facility for Testing Hydrodynamic Thrust Bearings, Proc Instn Mech Engrs Part J: J Engineering Tribology 216 (2002) 105-116.
10. Swanson, E.E., Kirk, R.G., Survey of Experimental Data for Fixed Geometry Hydrodynamic Journal Bearings, Journal of Tribology 119 (1997) 704-410.

## NOMENCLATURE

$b$	=	width of bearing
$c_p$	=	specific heat of lubricant
$e$	=	eccentricity
$f$	=	friction coefficient
$F_b$	=	friction force, surface b
$F_o$	=	cylinder load
$F_N$	=	bearing total load (= $w_r$ )
$h$	=	lubricant film thickness
$h_o$	=	minimum film thickness
$h_p$	=	power loss
$K$	=	power loss factor
$M$	=	friction torque

- $n$  = shaft rotating speed (rps)  
 $p$  = fluid film pressure  
 $p_{pro}$  = projected pressure ( $w_r / (2r_b * b)$ )  
 $P$  = pressure  
 $q_{in}$  = inlet flow rate of lubricant  
 $Q$  = flow rate of lubricant
- $r_b$  = shaft radius  
 $t$  = time  
 $T$  = temperature  
 $T_e$  = effective temperature  
 $T_{in}$  = inlet temperature  
 $\Delta T$  = lubricant temperature rise  
 $u_b$  = sliding speed in the x-direction  
 $w_r$  = bearing total load
- $x$  = coordinate in the direction of sliding motion  
 $x_1$  = coordinate along line of centers  
 $x_2$  = coordinate perpendicular to line of centers  
 $y$  = coordinate, bearing width direction
- $\eta_e$  = effective absolute viscosity  
 $\rho$  = lubricant density  
 $\phi$  = coordinate, ( $x / r_b$ )  
 $\Phi$  = attitude angle  
 $\omega$  = shaft rotation speed